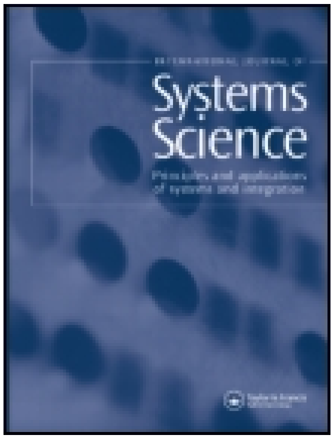

International Journal of Systems Science
Publication details, including instructions for authors and subscription information:
http://www.tandfonline.com/loi/tsys20

Fuzzy model-based fault detection and diagnosis for a pilot heat exchanger

Hacene Habbi [a] , Madjid Kidouche [a] , Michel Kinnaert [b] & Mimoun Zelmat [a]

[a] Applied Automation Laboratory, F.H.C., University of Boumerdès, Av. de l'Indépendance , 35000 Boumerdès, Algeria

[b] Service d'Automatique et d'Analyse des Systèmes , Université Libre de Bruxelles , 50 Av. F.D. Roosvelt, B-1050 Brussels, Belgium

Published online: 23 Aug 2010.

International Journal of Systems Science
Vol. 42, No. 4, April 2011, 587–599

Taylor & Francis
Taylor & Francis Group

Fuzzy model-based fault detection and diagnosis for a pilot heat exchanger

Hacene Habbi[a*], Madjid Kidouche[a], Michel Kinnaert[b] and Mimoun Zelmat[a]

[a]*Applied Automation Laboratory, F.H.C., University of Boumerdès, Av. de l'Indépendance, 35000 Boumerdès, Algeria;*
[b]*Service d'Automatique et d'Analyse des Systèmes, Université Libre de Bruxelles, 50 Av. F.D. Roosvelt, B-1050 Brussels, Belgium*

(*Received 2 April 2008; final version received 15 January 2010*)

This article addresses the design and real-time implementation of a fuzzy model-based fault detection and diagnosis (FDD) system for a pilot co-current heat exchanger. The design method is based on a three-step procedure which involves the identification of data-driven fuzzy rule-based models, the design of a fuzzy residual generator and the evaluation of the residuals for fault diagnosis using statistical tests. The fuzzy FDD mechanism has been implemented and validated on the real co-current heat exchanger, and has been proven to be efficient in detecting and isolating process, sensor and actuator faults.

Keywords: fault detection and isolation; fuzzy identification; heat exchangers

1. Introduction

In many industrial applications, production processes are becoming more and more complex and therefore there is a growing demand for fault detection and diagnosis (FDD) in order to provide safe and continuous operation. Early and accurate detection and isolation of different types of faults (sensor, actuator and component faults) in operation mode is the major task that should be achieved by designing a fault diagnosis system. This may help in reducing possible damage to equipment and productivity loss, and consequently ensures safety for operators. Over the last two decades, model-based approaches to FDD in complex processes have been investigated in both the research context and also in the domain of application studies on real plants (Isermann 1984; Gertler 1988; Ballé, Juricic, Rakar, and Ernst 1997; Ballé and Fuessel 2000). Satisfactory performance of such approaches can only be achieved if reliable dynamic models with known properties and interpretable structure built from accumulated operational experience are available. However, the effect of modelling uncertainties, disturbances and noise is the most crucial point in the model-based FDD concept and the solution to this problem is the key for its practical applicability (Isermann 2005).

Heat exchangers are the subject under discussion in this article. They are important components in many industrial processes, for example, power and chemical industries, oil refineries and other areas. They are usually arranged in units containing several (5–200) of them. Common heat exchanger faults are tube and pipe leaks due to aging and thermal stress, temperature sensor faults and valve actuator faults.

From a mathematical modelling point of view, heat exchangers are nonlinear distributed parameter systems in which faults can be modelled by time-varying parameters or supplementary disturbance inputs (additional flows for leaks, for instance). The models can be built either from expert knowledge (first-principle based models) or from measured data (data-based models). A first-principle-based model allows a better understanding of the process behaviour and then a greater depth in diagnosis, due to the interpretable parameters. However, physical models of heat exchangers are difficult to derive by theoretical modelling since the underlying physical effects are quite complex and a certain number of system parameters, such as heat transfer coefficients, are unknown (Weyer, Szederkenyi, and Hangos 2000; Persin and Tovornik 2005; Astorga-Zaragoza, Alvarado-Martinez, Zavala-Rio, Mendez-Ocana, and Gaerrero-Ramrez 2008).

In addition to sensor and actuator faults, tube and pipe leaks in heat exchangers are a special type of process faults which belong to the class of gross error problems (Sun, Chen, and Marquez 2002). They can induce significant effects on the process transient behaviour and then the use of steady-state models or linear models will not have many practical implications. An efficient method to obtain the required

*Corresponding author. Email: habbi_hacene@hotmail.com

ISSN 0020–7721 print/ISSN 1464–5319 online

DOI: 10.1080/00207721003653666
http://www.informaworld.com

nonlinear dynamic models is to resort to models based on fuzzy logic reasoning. This rule-based modelling paradigm has recently become an effective and attractive solution to a wide range of systems identification problems (Skrjanc and Matko 2000; Habbi, Zelmat, and Ould Bouamama 2003). The present contribution shows how multivariable fuzzy models are built and used to cope with the fault detection and isolation problem in a pilot thermal plant.

To build the fuzzy model-based FDD system, a three-step procedure is applied. In the first stage, a nonlinear dynamic multi-input–multi-output (MIMO) fuzzy model of the real pilot plant is identified from input–output observations collected in a normal operation using a fuzzy clustering technique. The second step consists of the design of a nonlinear residual generator using a bank of fuzzy models, all of them identified from healthy measured data. This is a filter that uses actual plant measurements and actuator commands to generate symptoms in the form of residual signals. These detection signals have the property of being approximately zero in a fault-free situation and some of them deviate from zero upon the occurrence of a fault. The third step is the design of the decision module. The decision procedure being used in our application study relies on Hinkley's cumulative sum (CUSUM) algorithm (Blanke, Kinnaert, Lunze, and Staroswiecki 2003). The idea consists of detecting online changes in the statistics of the residual sequences based on an optimal decision function. The validation of the FDD algorithm is performed on the pilot heat exchanger and its design parameters are determined via simulations using the real data collected during the experimental study.

Briefly, this article is organised as follows. After reviewing the multivariable fuzzy modelling concept in Section 2, the description and fuzzy identification of the pilot heat exchanger are presented in Section 3. Sections 4 and 5 address the design of the fuzzy model-based FDD scheme and Section 6 discusses its implementation issues and gives the experimental diagnosis results. Finally, concluding remarks are given in Section 7.

2. Fuzzy identification by means of data clustering

2.1. *Multivariable fuzzy models*

Fuzzy rule-based models are often used to model systems in an input–output sense by means of IF–THEN rules. Data-driven fuzzy identification is an effective tool for building fuzzy models that can approximate any continuous function on a compact set to an arbitrary precision (Cao, Rees, and Feng 1997). So far, most attention has been devoted to the fuzzy identification of multi-input–single-output (MISO) systems, but MIMO systems have also been investigated, mostly in connection to MISO structures (Babuška, Roubos, and Verbruggen 1998).

The pilot heat exchanger under study in the present contribution is typically an uncertain nonlinear MIMO system and the identification of its MIMO fuzzy model for FDD purposes is achieved by means of fuzzy clustering. To be able to present the theoretical aspects of the general fuzzy identification procedure, let us consider a MIMO system with r inputs, $u \in U \subset \Re^r$, and m outputs, $y \in Y \subset \Re^m$. This system can be approximated by a set of coupled MISO fuzzy models that are of input–output nonlinear autoregressive with exogenous input (NARX) type:

$$y_l(k) = \mathcal{F}_l(\varphi_l(k)), \quad l = 1, 2, \dots, m, \tag{1}$$

where the regression vector $\varphi_l(k)$ is given by

$$\begin{aligned}\varphi_l(k) = [&u_1(k-1), \dots, u_1(k-n_{ul1}), \dots, \\ &u_r(k-1), \dots, u_r(k-n_{ulr}), \\ &y_1(k-1), \dots, y_1(k-n_{yl1}), \dots, \\ &y_m(k-1), \dots, y_m(k-n_{ylm})]^T.\end{aligned} \tag{2}$$

Here $n_{ul1}, \dots, n_{ulr}$ and $n_{yl1}, \dots, n_{ylm}$, $l = 1, \dots, m$, represent the dynamic orders of the inputs and the outputs, respectively. The nonlinear functions $\mathcal{F}_l(\cdot)$ are known only at the available data samples and each function will be approximated by a rule-based fuzzy model of the Takagi–Sugeno (TS) type (Driankov, Hellendoorn, and Reinfrank 1993) with c_l fuzzy rules of the form:

$$\begin{aligned} R_l^i:\quad &\text{If } x_{l1}(k) \text{ is } A_{l1}^i \text{ and } x_{l2}(k) \text{ is } A_{l2}^i \text{ and} \dots \\ &\text{and } x_{ln}(k) \text{ is } A_{ln}^i \\ &\text{then } y_l^i(k) = a_{l1}^i x_{l1}(k) + \dots + a_{ln}^i x_{ln}(k) + b_l^i \\ &\quad i = 1, \dots, c_l; \quad l = 1, \dots, m, \end{aligned} \tag{3}$$

where $\mathrm{x}_l(k) = [x_{l1}(k)\ x_{l2}(k) \dots x_{ln}(k)]^T \subseteq \varphi_l(k)$ is a vector containing subsets of the process input and output variables and A_{lj}^i, $(1 \le j \le n)$, is a fuzzy set defined on the universe of discourse of the rule-premise variable x_{lj} in the lth TS fuzzy model. The rule consequents are typically linear functions with constant parameters a_{lj}^i and offsets b_l^i. In the sense of a discrete transfer function, the rule-consequent in the lth model describes a local linear process behaviour.

Choosing the product operator as t-norm, the output of the TS fuzzy model is computed by the weighted mean:

$$y_l(k) = \frac{\sum_{i=1}^{c_l} \mu_{li}(\mathrm{x}_l(k))\, y_l^i(k)}{\sum_{i=1}^{c_l} \mu_{li}(\mathrm{x}_l(k))}, \quad l = 1, 2, \dots, m. \tag{4}$$

In the input–output product space, $\mu_{li}(\mathrm{x}_l(k))$ is simply the activation degree of the ith rule in the lth TS fuzzy model which is given by the product of the individual antecedent membership degrees in the conjunctive form (3), i.e.

$$\mu_{li}(\mathrm{x}_l(k)) = \prod_{j=1}^{n} \mu_{A^i_{lj}}(x_{lj}(k)), \quad l = 1, 2, \ldots, m, \tag{5}$$

where $\mu_{A^i_{lj}}(x_{lj}) : \Re \to [0, 1]$ is the membership function of the fuzzy set A^i_{lj} in the antecedent of the rule R^i_l of the lth TS fuzzy model.

The structure of the fuzzy model, i.e. the integers $n_{ul1}, \ldots, n_{ulr}$ and $n_{yl1}, \ldots, n_{ylm}$, and the components of the regression vectors $\mathrm{x}_l(k)$, are determined on the basis of prior knowledge and/or by comparing several candidate structures in terms of the prediction error or other suitable criteria (Sugeno and Yasukawa 1993). This may help in building interpretable fuzzy models with appropriate validity regions (Johansen, Shorten, and Smith 2000). Once the structure is fixed, the rule-premise and the rule-consequent parameters of the MISO models (3) including the number of fuzzy rules are all estimated by means of data clustering. In this work, the MISO models are identified independently of each other using the well-established Gustafson–Kessel (GK) fuzzy clustering algorithm (Gustafson and Kessel 1978), which is described in the following section.

2.2. *Gustafson–Kessel fuzzy clustering*

The GK fuzzy clustering algorithm, which is the fuzzy generalisation of the adaptive distance dynamic clusters (ADDC) algorithm (Zhao, Wertz, and Gorez 1994), achieves data set partitioning into fuzzy sets. It uses an adaptive distance measure that allows detection of hyper-ellipsoidal clusters with different shapes and different orientations (Babuška and Verbruggen 1996). This algorithm splits the identification procedure into two parts: the generation of the premise structure and the corresponding membership functions, respectively, and the estimation of the parameters of the local linear models by a weighted least-squares algorithm.

To identify the MIMO fuzzy model, the regression matrix X and an output vector y_s are constructed from the available input–output data sequences:

$$\mathrm{X}^T = [\mathrm{x}(1), \ldots, \mathrm{x}(N)], \quad \mathrm{y}_s^T = [y(1), \ldots, y(N)], \tag{6}$$

where N is the number of samples. The regression data (6) is built for each of the m MISO models, but here, for the sake of brevity, the output index l will be omitted.

The data set Z to be clustered is formed by concatenating y_s to $\mathrm{X}: \mathrm{Z}^T = [\mathrm{X}, \mathrm{y}_s]$, where each column $\mathrm{z}(k)$, $k = 1, 2, \ldots, N$, of Z contains an input–output data pair: $\mathrm{z}(k) = [\mathrm{x}^T(k), y(k)]^T$. Thus, given $\mathrm{Z} \in \Re^{(n+1)\times N}$ and the estimated number of clusters c, the GK fuzzy clustering algorithm is applied. This algorithm computes in an iterative manner the fuzzy partition matrix $\mathrm{U} = [\mu_{ik}]_{c\times N}$, with $\mu_{ik} \in [0, 1]$, the cluster prototype matrix $\mathrm{V} = [\mathrm{v}_1, \ldots, \mathrm{v}_c]$, $\mathrm{v}_i \in \Re^{n+1}$ and the covariance matrices $\mathrm{F} = [\mathrm{F}_1, \ldots, \mathrm{F}_c]$, $\mathrm{F}_i \in \Re^{(n+1)\times(n+1)}$, all of them result from a nonlinear optimisation problem based on the squared inner-product-induced distance

$$d^2_{ki} = (\mathrm{z}(k) - \mathrm{v}_i)^T D_i (\mathrm{z}(k) - \mathrm{v}_i), \tag{7}$$

where the norm-inducing matrix D_i is obtained from the covariance of the clusters (Babuška et al. 1998). Then, in order to obtain the membership functions for fuzzy sets A^i_j, $1 \le j \le n$, of the conjunctive form (3), the multi-dimensional fuzzy sets defined point-wise in the ith row of the partition matrix U can be projected onto the regressors x_j by

$$\mu_{A^i_j}(x_j(k)) = \mathrm{proj}_j(\mu_{ik}), \tag{8}$$

where proj is the point-wise projection operator (Babuška et al. 1998; Simani, Fantuzzi, and Patton 2002). The point-wise defined fuzzy sets A^i_j are then approximated by a suitable parametric function.

The step that follows the model structure identification consists of the estimation of the rule-consequent parameters. These parameters can be computed using global or local weighted ordinary least-square methods. More precisely, let $\theta_i^T = [\mathrm{a}_i^T, b_i]$, where $\mathrm{a}_i^T = [a^i_1, \ldots, a^i_n]$, let $\mathrm{X}_e = [\mathrm{X}, 1]$ and let W_i denote a diagonal matrix in $\Re^{N\times N}$ having the degree of activation μ_{ik} as its kth diagonal element. If the columns of X_e are linearly independent and $\mu_{ik} > 0$ for $k = 1, \ldots, N$, then

$$\theta_i = [\mathrm{X}_e^{\mathrm{T}} \mathrm{W}_i \mathrm{X}_e]^{-1} \mathrm{X}_e^{\mathrm{T}} \mathrm{W}_i \mathrm{y}_s, \quad i = 1, 2, \ldots, c \tag{9}$$

is the local weighted least-squares solution to the parameter estimation problem (Setnes 2000). In contrast to the global estimation, this local parameter estimation method can be seen as a special form of regularisation (Fink, Fischer, Nelles, and Isermann 2000). It helps in avoiding compensation effects that deteriorate the validity of the local models in the identified operating regions.

3. Process description and fuzzy modelling

3.1. *Process description*

The process under investigation is a co-current heat exchanger, which is the main part of the pilot plant depicted in Figure 1. It consists of three

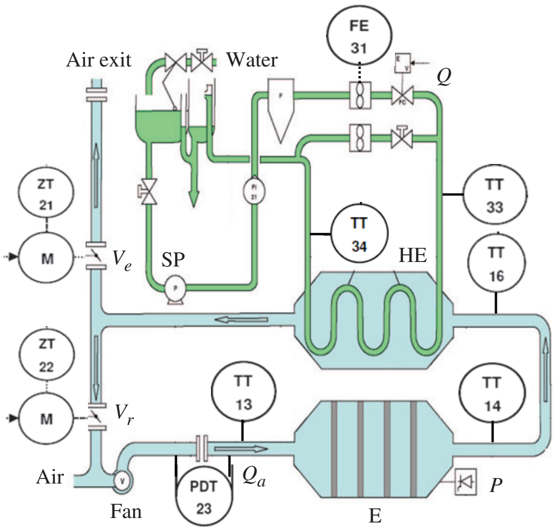

Figure 1. Schematic representation of the pilot heat exchanger.

subsystems: the heater, the air circuit and the water circuit. In more detail, the system is composed of an electric heater of the air (E), pipes for air and water circulation, a co-current gas-liquid exchanger (HE), two valves, (V_r) and (V_e), to control the portion of the air flow that is recycled and the portion that is evacuated and a variable speed pump (SP) to control the water flow. The water entering the heat exchanger with the temperature T_{33} is heated up to the temperature T_{34} with hot air. The amount of air coming from the electric heater with temperature T_{14} enters the heat exchanger with the temperature T_{16} after flowing through the air circulation pipe. Total or partial recycling of air can be considered depending on the position of the two motor-driven valves V_r and V_e. This allows the emphasising of different operation modes of the heat exchanger in the experimental study.

The following variables can be measured:

- P — the heating power (kW);
- T_{14} and T_{16} — the air temperature, respectively, after the heater and before the heat exchanger (°C);
- T_{33} and T_{34} — the water temperature, respectively, at the inlet and the outlet of the heat exchanger (°C);
- V_r and V_e — the position of the air recycling valve and the air evacuation valve, respectively (%);
- Q_a — the air flow rate (m^3/s);
- Q — the water flow rate (m^3/s).

A bypass valve situated in the water circulation pipe can be used to simulate leak faults in the heat exchanger. By adjusting its position, a single-leak flow from 0 to 80 L/h can be introduced on the real plant. For the FDD system design, the major task is to find a supervision scheme for some relevant measured variables based on model equations and no additional sensor signals.

3.2. *Fuzzy modelling of the heat exchanger*

As mentioned above, the FDD system presented in this contribution is based on a data-driven MIMO fuzzy model of the pilot heat exchanger. The model is built by means of a fuzzy identification algorithm from measurement data. The main task is to find a suitable and transparent fuzzy model structure for the co-current heat exchanger that can predict its nonlinear behaviour accurately over a wide operating range. For this purpose, both water and air circuits of the thermal plant are considered. Due to physical considerations, it is clear that the normal input–output behaviour of each circuit depends mainly on the heating power P, the air recycling valve position V_r, the air evacuation valve position V_e, the air temperature before the heat exchanger T_{16}, the air temperature at the outlet of the heater T_{14} and the water temperature after the heat exchanger T_{34}. The structure of the global MIMO fuzzy model to be identified will then involve all of these physical variables. Simple experiments recording the time-step responses of the air circuit and the water circuit show us the principal local behaviour of the heat exchanger. From these experiments we concluded that there is no evidence for higher than first-order local dynamics. Therefore, we need to find a supervision scheme for the five measurements of T_{34}, T_{16}, T_{14}, P, V_r, based on the following NARX model structure:

$$\begin{cases} T_{34}(k+1) = \mathcal{F}_1(T_{34}(k), T_{16}(k), P(k), V_r(k)), \\ T_{16}(k+1) = \mathcal{F}_2(T_{16}(k), T_{14}(k), P(k), V_r(k)), \end{cases} \tag{10}$$

where $\mathcal{F}_1(\cdot)$ and $\mathcal{F}_2(\cdot)$ are unknown nonlinear functions.

To identify this multivariable fuzzy model, the nonlinear functions in Equation (10) must be approximated by a set of IF–THEN fuzzy logical rules with functional consequent parts. More precisely, a TS-type fuzzy model is to be identified for each circuit in normal operation mode. To this end, real data from the pilot heat exchanger are generated in the fault-free situation where the air flow rate Q_a supplied by a fan and the water flow rate Q are both kept constant. The heating power is manipulated over its whole operating domain from 0 to 10 kW. The air recycling valve position V_r and the air evacuation valve position V_e are controlled simultaneously in the range 0–100%.

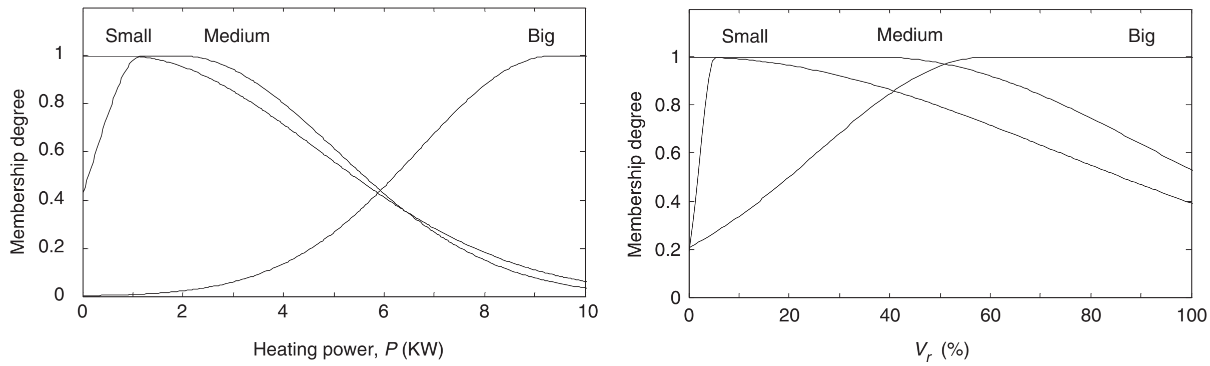

Figure 2. Membership functions for the premise inputs P and Vr for T_{34} prediction model.

These three variables represent the manipulated variables. To ensure the safety of the pilot plant during the identification experiment, the following working condition is considered:

$$V_r(k) = 100\% - V_e(k). \tag{11}$$

The dependency between V_r and V_e expressed by Equation (11) explains the use of V_r only as a regressor in system (10). Also, since we need to consider large variations of the process operating point, we used dynamic excitations in the heating power, P, and in the valve positions, V_r and V_e, by employing amplitude-modulated pseudo-random binary signals. The system was sampled every 2 s. This sampling period is chosen with respect to the air circuit time constant, which is faster than the water circuit time constant. The MIMO fuzzy model structure used for the simultaneous prediction of the water temperature T_{34} and the air temperature T_{16} is described by a set of IF–THEN fuzzy rules of the form:

$$\begin{aligned}
R_1^i\colon &\text{IF } P(k) \text{ is } A_{11}^i \text{ and } V_r(k) \text{ is } A_{12}^i \text{ and } T_{16}(k) \\
&\quad \text{is } A_{13}^i \text{ and } T_{34}(k) \text{ is } A_{14}^i \\
&\text{THEN } T_{34}(k+1) = b_1^i + a_{11}^i P(k) + a_{12}^i V_r(k) \\
&\quad + a_{13}^i T_{16}(k) + a_{14}^i T_{34}(k) \\
&\text{ALSO} \\
R_2^i\colon &\text{IF } P(k) \text{ is } A_{21}^i \text{ and } V_r(k) \text{ is } A_{22}^i \text{ and } T_{14}(k) \\
&\quad \text{is } A_{23}^i \text{ and } T_{16}(k) \text{ is } A_{24}^i \\
&\text{THEN } T_{16}(k+1) = b_2^i + a_{21}^i P(k) + a_{22}^i V_r(k) \\
&\quad + a_{23}^i T_{14}(k) + a_{24}^i T_{16}(k).
\end{aligned} \tag{12}$$

One can see that for each model output, the four regressors defined in Equation (10) are all involved in the rule-antecedents of the MIMO fuzzy model (12). This may allow a better understanding of the transfer behaviour between the rule premise inputs and the process output temperatures.

3.2.1. *Identification results*

The GK fuzzy clustering algorithm described in Section 2 is applied to the set of fault-free input–output observations which contains 2000 samples. The number of clusters to be detected for each MISO model is $c_l = 3$, $l = 1, 2$, and as so, the global MIMO fuzzy model of the heat exchanger has six rules. This number is determined by clustering the real data for different values of c_l, $(c_l = 2, 3, 4, \dots)$ and using the variance accounted for (VAF) index to assess the goodness of the obtained model structure. The VAF is a widely used validity measure, which is defined as (Babuška et al. 1998)

$$\text{VAF} = \frac{1 - \text{var}(y_l - \hat{y}_l)}{\text{var}(y_l)} \times 100\%, \tag{13}$$

where y_l is the real process output, $\hat{y}_l$ is the model output and var(·) is the variance of the respective vector. When VAF is close to 100%, the model is then very accurate, as desired, which explains all the variability in the real outputs.

The resulting input space partitioning of the heating power and the air recycling valve position for T_{34} prediction corresponds to the membership functions depicted in Figure 2. These fuzzy sets are labelled as Small (S), Medium (M) and Big (B), and then define three operating regions for each manipulated variable. Note that any further increase in the model complexity does not improve the MIMO fuzzy model performance.

To assess its performance, the identified fuzzy model is first run in parallel configuration to the real process using the training data. The results are shown in Figure 3. One can notice easily the good matching between the process outputs and the fuzzy model outputs. This performance is maintained even during the saturation of the air temperature T_{16}, which is an important feature of the developed fuzzy model. This demonstrates the approximation capability of the

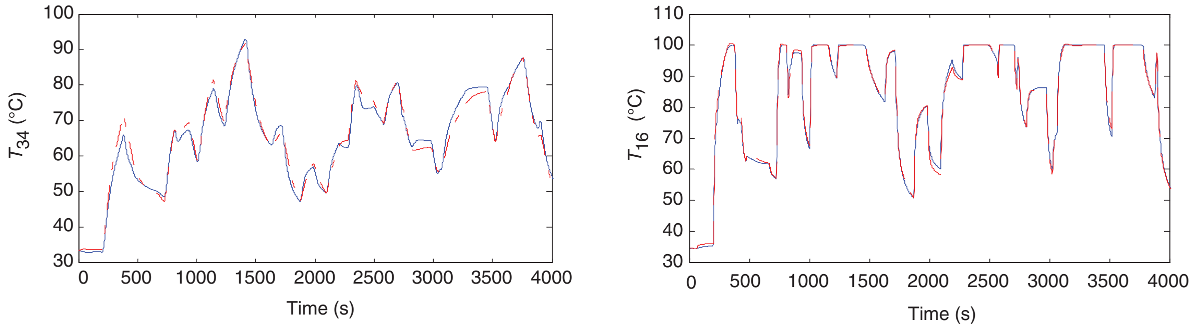

Figure 3. Performance of the MIMO fuzzy model with training data: real process outputs (solid), fuzzy model outputs (dashed).

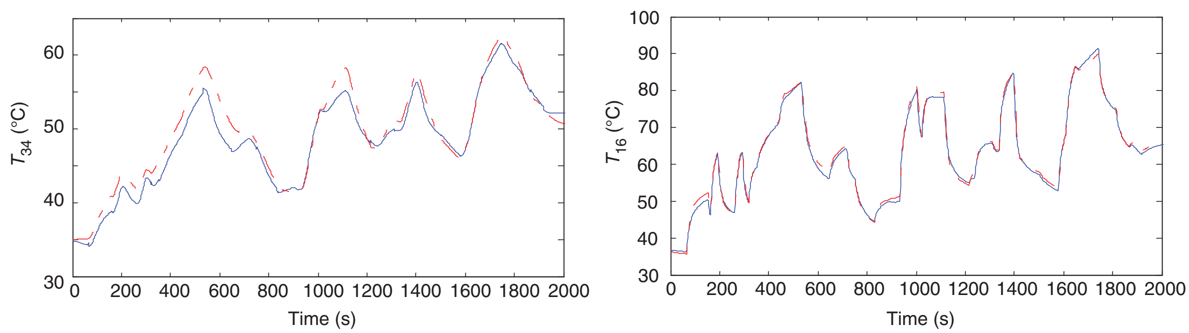

Figure 4. Performance of the MIMO fuzzy model with validation data: real process outputs (solid), fuzzy model outputs (dashed).

proposed fuzzy model. For validation, a second input data set, different from the one used in the identification experiment, is applied to the real plant. The performance of the fuzzy model on validation data is depicted in Figure 4. For evaluating the overall model performance, the mean-square error (MSE) index is used:

$$\mathrm{MSE} = \frac{1}{N}\sum_{k=1}^{N}[y_l(k) - \hat{y}_l(k)]^2, \tag{14}$$

where N is the number of data samples, and y_l and $\hat{y}_l$ are as defined in Equation (13). Table 1 shows the model performance obtained in parallel and series–parallel configurations using both identification and validation signals. The resulting MSEs are all close to zero, which is a key feature in the model-based FDD concept.

Table 1. Fuzzy model performance (mean-square error).

		Identification signal		Cross validation signal	
Predicted output	Local models	p	s	p	s
T_{34}	3	0.0421	0.0001	0.0292	0.00008
T_{16}	3	0.0097	0.0013	0.0087	0.00094

Note: p – parallel model, s – series-parallel model.

Moreover, it must be noticed that, due to the different structure, the derived model performance based on both configurations (parallel and series–parallel) shows different results. For the series–parallel model, the measured noisy process output is fed-back instead of the noise-free estimated one. Hence, the signal-to-noise ratio is smaller (Ballé 1999). The output signal contains information about the process output, and therefore the model is adapted to the actual process state and has a better performance. However, this leads to residual signals that are less sensitive or almost insensitive to faults. Consequently, a fault decision becomes impossible. On the other hand, the parallel model has an internal feedback and therefore is likely to drift due to model uncertainties. But for fault detection, it leads to residuals that are sensitive to faults, as will be shown in the next section.

4. Residual generation

The general FDD scheme is based on the comparison of measured process output temperatures and

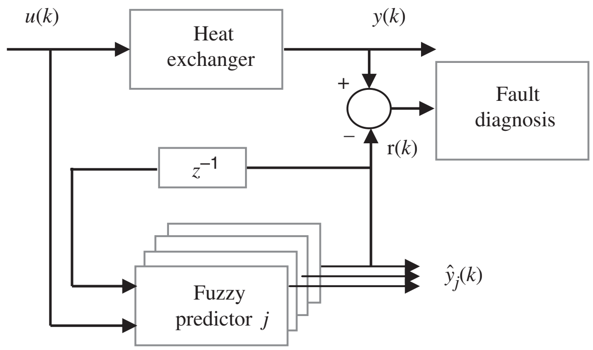

Figure 5. General fuzzy model-based FDD.

estimated temperatures provided by a bank of fuzzy predictors as depicted in Figure 5. It consists of the blocks symptom generation and fault diagnosis through residual evaluation. In the experimental study, the following faults were considered:

- f_ϕ leak in the water circulation pipe;
- $f_{T_{34}}$ bias of the sensor for T_{34} measurement;
- $f_{T_{16}}$ bias of the sensor for T_{16} measurement;
- f_p actuator fault in heating power;
- f_V air recycling valve blockage.

The generation of residuals is achieved with the aid of the identified nonlinear MIMO fuzzy model (12) that is run in parallel to the real process. The residual signals we only need to generate for fault detection purpose are $r_{T_{34}}$ and $r_{T_{16}}$ which correspond to the differences between the real process outputs $\mathrm{y}(k) = [T_{34}(k)\ T_{16}(k)]^T$ and the fuzzy model outputs $\hat{\mathrm{y}}(k) = [\hat{T}_{34}(k)\ \hat{T}_{16}(k)]^T$. This means that a change in the water temperature or in the air temperature is required to detect the anomaly. Hence, the residual vector is computed within a time window as

$$\mathrm{r}(k) = \mathrm{y}(k) - \hat{\mathrm{y}}(k). \tag{15}$$

These detection signals have the property of being approximately zero in the normal (fault-free) situation. In the ideal case (perfect modelling and fault-free), r(k) consists of measurement noises only, which can be assumed to be zero mean. However, in reality, many temporary or time-varying disturbances exist. This will in turn result in r(k) that may not be zero mean statistically and may change with time.

The isolation of the considered faults is not feasible with only supervising the water and air temperatures estimated by the MIMO fuzzy model (12). Indeed, it is necessary to construct additional fuzzy predictors from the healthy input–output observations so that more than two residual signals, with specific properties, can be generated. More precisely, six structured residuals including the two residual signals generated on the basis of the MIMO fuzzy model (12) are determined. The additional four residuals are constructed using a bank of TS fuzzy models, all of them identified from fault-free measurement data using the GK fuzzy clustering algorithm. For each fuzzy predictor, the same identification procedure, described in Section 2, is applied. The excitation signals used in the experiments cover the whole operating domain of the heat exchanger variables. To guarantee a unique pattern for each fault in this multi-model approach, appropriate structures are determined. Here, expert knowledge and operator's experience were of major importance to define the structure of each fuzzy predictor and the relevant measurements. The designed fuzzy predictors are summarised in Table 2. Note that $\xi_j(\cdot)$, $j = 1, 2, \ldots, 6$, stand for nonlinear dynamic functions of the physical inputs. Table 2 also presents the model performance and the number of local models.

Table 2. Structure and performance of the designed fuzzy predictors.

Fuzzy predictor	Structure	Local models	Performance (MSE)	Residual
1	$T_{34} = \xi_1(T_{34}, T_{16}, P, V_r)$	3	0.0421	r_1
2	$T_{34} = \xi_2(T_{34}, T_{14}, P, V_r)$	3	0.0184	r_2
3	$T_{34} = \xi_3(T_{34}, T_{16}, P)$	3	0.0636	r_3
4	$T_{34} = \xi_4(T_{34}, T_{16}, V_r)$	3	0.1023	r_4
5	$T_{16} = \xi_5(T_{16}, T_{14}, P, V_r)$	3	0.0097	r_5
6	$T_{16} = \xi_6(T_{16}, T_{14}, P)$	3	0.0122	r_6

Table 3. Incidence matrix.

Residual	$f_{T_{34}}$	$f_{T_{16}}$	f_P	f_V	f_ϕ
r_1	1	1	1	1	1
r_2	1	0	1	1	1
r_3	1	1	1	0	1
r_4	1	1	0	1	1
r_5	0	1	1	1	0
r_6	0	1	1	0	0

The fault pattern can be depicted in the incidence matrix shown in Table 3. In this incidence matrix, a '1' in the ith row and the jth column indicates that residual r_i is sensitive to the jth fault, while '0' denotes insensitivity. Note that, since process fault type is emphasised, not only the fact that a residual is deflected, but also the direction of deflection is of interest. Indeed, both f_ϕ and $f_{T_{34}}$ affect the behaviour of the residual $r_{T_{34}}$, which leads to a similar fault pattern, as can be seen in Table 3. However, at steady state, a leak fault can induce only positively directed residuals (measurement larger than estimation),

Table 4. Residual patterns resulting from leak faults.

Residual fault	r_1	r_2	r_3	r_4	r_5	r_6
$f_\phi = 25\%$ $k_0 = 950$ $(t = 1900\,\text{s})$	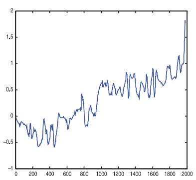	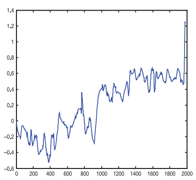	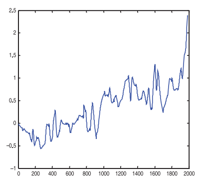	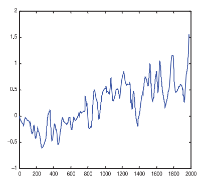	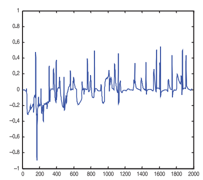	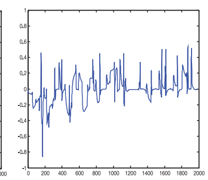
$f_\phi = 30\%$ $k_0 = 640$ $(t = 1280\,\text{s})$	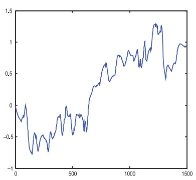	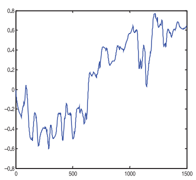	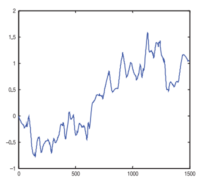	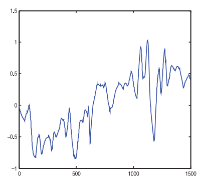	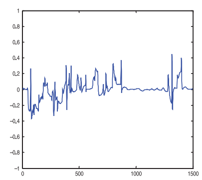	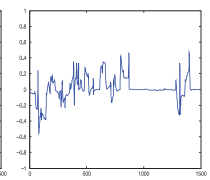
$f_\phi = 40\%$ $k_0 = 290$ $(t = 580\,\text{s})$	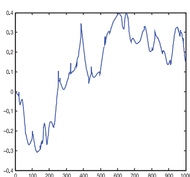	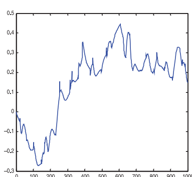	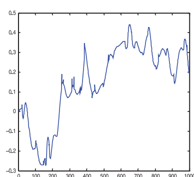	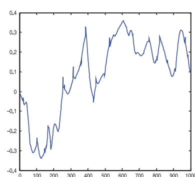	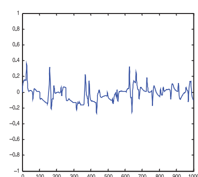	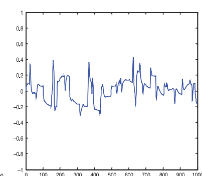

which may help in making an adequate decision on fault occurrence during the residual evaluation step.

4.1. *Validation of the fuzzy residual generator*

To analyse the sensitivity of the residuals to the considered types of process, sensor and actuator faults, experiments on the real plant were performed. Only single faults are emphasised under varying excitation signals on heating power P and air recycling and evacuation valve positions V_r and V_e. These manipulated variables are, in most cases, changed over the whole operating range but kept, in some leak test cases, in a limited range with respect to the magnitude of the simulated leak fault. The process data and the residuals were captured for 2000 s, 3000 s or 4000 s, depending on the test case, while the faults were generated in specific time periods. Table 4 shows the residual patterns obtained for single-leak faults with magnitudes 25%, 30% and 40% introduced at time instant $t = 1900\,\text{s}$, $t = 1280\,\text{s}$ and $t = 580\,\text{s}$, respectively, using a bypass valve situated in the water circulation pipe of the heat exchanger. The validity of the steady-state behaviour summarised in Table 3 can be checked from Table 4. It appears that, after a transient phase, the measured water temperature T_{34} and the residuals r_1, r_2, r_3 and r_4 rise, because a smaller volume of water is heated up with the same amount of air supplied in normal operation. Also, it can be seen that for 40% leak case, although the leak magnitude is big, the water temperature T_{34} has not risen sufficiently and then the change in the mean value of the corresponding residuals is not significant enough as could be expected. This is due to the weak excitation in the heating power, P, which was applied to the heat exchanger in this experiment. Indeed, because 40% is a considerable leak flow, it was necessary to prevent the pilot plant from any damage after leak occurrence. However, one should not consider this result as a limitation on the validity of the identified fuzzy predictors. Indeed, better deductions could be made under these considered working conditions if the experiment was extended enough in time (much more than 1000 data samples). Obviously, the air temperature T_{16} is not affected by the leak faults. The corresponding residuals r_5 and r_6 are almost zero and consist only of measurement noise.

Table 5 shows the residual patterns for single sensor and actuator faults introduced separately at different time instants. More precisely, an offset of 4°C is added from $t = 3000\,\text{s}$ to the measured values of T_{34} and from $t = 2000\,\text{s}$ to the measured values of T_{16}. Next, to simulate actuator faults, we considered the blockage of the recycling valve V_r by keeping it fully closed from $t = 1000\,\text{s}$, and a fault in the heating power actuator by adding an offset of 2 kW to P from

Table 5. Residual patterns resulting from sensor and actuator faults.

Residual fault	r_1	r_2	r_3	r_4	r_5	r_6
$f_{T_{34}} = 4°C$ $k_0 = 1500$ ($t = 3000$ s)	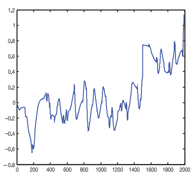	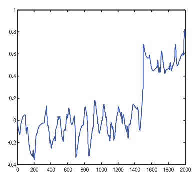	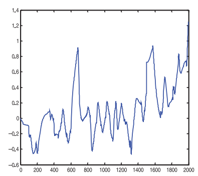	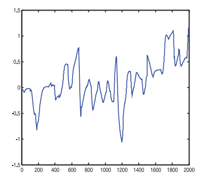	0	0
$f_{T_{16}} = 4°C$ $k_0 = 1000$ ($t = 2000$ s)	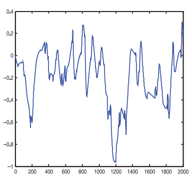	0	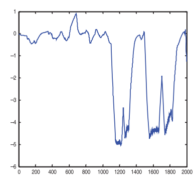	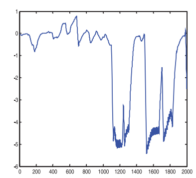	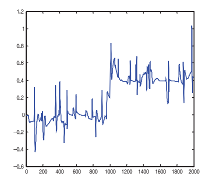	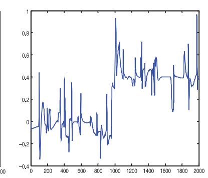
$f_P = 2$ kW $k_0 = 500$ ($t = 1000$ s)	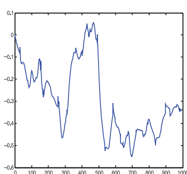	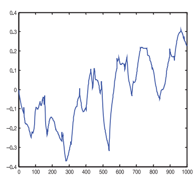	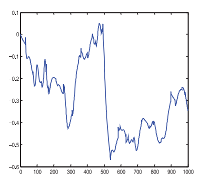	0	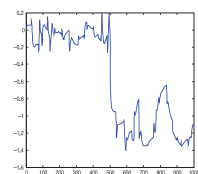	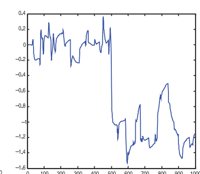
f_V (closed) $k_0 = 500$ ($t = 1000$ s)	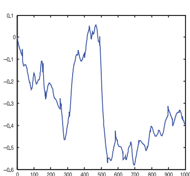	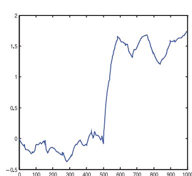	0	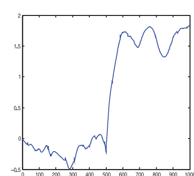	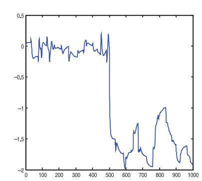	0

$t = 1000$ s. As the plant inputs are changed, the real measurements taken in the absence of actuator faults are no longer valid. From the plots shown in Table 5, it appears that some residuals exhibit significant deflection after fault occurrence, while it is quite difficult to distinguish clearly the deviation in some few cases due to modelling uncertainties and unknown inputs.

This is particularly for residual r_1 in fault case $f_{T_{16}}$ and residuals r_3 and r_4 in fault case $f_{T_{34}}$. The sensitivity of the overall FDD scheme is generally evaluated using the most sensitive residual signals.

5. Decision system

The diagnosis block plays the role of monitoring the residual set described previously. It processes the generated residual sequences based on an appropriate decision logic. Generally, to evaluate the residuals, alarm thresholds should be set up for r(k). The selection of suitable alarm thresholds is important: small thresholds will enhance the sensitivity of the fault detection algorithm, but false alarms will also increase; on the other hand, large thresholds will result in missing some faults. However, in practice, for some residuals the signal-to-noise ratio is small so that a decision procedure based on the comparison of these signals to thresholds is not feasible. This is particularly the case for slowly developing leak faults, and sensor and actuator faults with weak magnitudes. Of course, one could filter the residuals before comparing them to a threshold, but this is precisely what probabilistic approaches do implicitly in an optimal way (Basseville and Nikiforov 1993).

The decision procedure we used in our application study relies on Hinkley's CUSUM algorithm. This choice is justified by the fact that most of the simulated single faults have induced a visible change in the mean of the symptom signals. Theoretically, for applying the CUSUM algorithm, the successive samples of these signals should be independent, which is not fulfilled here. However, the robustness of the algorithm with respect to this condition is known to hold in practice (Kinnaert, Vrancic, Denolin, Juricic, and Petrovicic 2000).

To be able to present this approach, let us consider the sequential observation of the q-dimensional residual vector $\mathrm{r}(k)$ with probability density function depending upon a q-dimensional vector ν which represents the mean of the residual vector in our case. Before an unknown change time, k_0, ν is equal to $\nu_0 \approx 0$. At time k_0, it changes to $\nu = \nu_\ell \neq \nu_0$ under the effect of a fault of type ℓ, $\ell = 1, \ldots, 5$. The aim is then to detect the transition from a healthy mode in which $\nu = \nu_0$ holds to a faulty situation where $\nu = \nu_\ell$ is fulfilled. More precisely, the change detection algorithm must provide a pair $(k_a, \hat{k}_0)$ where k_a is the alarm time and $\hat{k}_0$ an estimate of the fault occurrence time. The residual vector is assumed to be Gaussian-type and thus its distribution is

$$\mathcal{L}(\mathrm{r}(k)) = \begin{cases} \mathcal{N}(\nu_0, \Sigma) & \text{in the fault-free mode,} \\ \mathcal{N}(\nu_\ell, \Sigma) & \text{in the } \ell\text{th fault mode.} \end{cases} \tag{16}$$

The estimates of the mean value ν_0 and the variance Σ of the residual sequence $\mathrm{r}(k)$ can be obtained from the collected fault-free data samples. The fault effects characterised by vectors ν_ℓ, $\ell = 1, \ldots, 5$, are assumed to be known. In our case study, the vectors ν_ℓ are determined through several experiments conducted for each fault type ℓ. This is obviously not always possible to achieve in most of the practical situations. Yet, the CUSUM algorithm has been shown to perform well even when the fault magnitudes are different from the assumed ones (Kinnaert et al. 2000).

Hypothesis $\mathcal{H}_0$ is said to hold when the residual vector has distribution $\mathcal{N}(\nu_0, \Sigma)$, while hypothesis $\mathcal{H}_\ell$ is associated to the situation where the residual has distribution $\mathcal{N}(\nu_\ell, \Sigma)$. From classical results in hypothesis testing due to Neyman and Pearson (Blanke et al. 2003), it is known that tests to decide between the fault-free situation ($\mathcal{H}_0$) and the faulty one ($\mathcal{H}_\ell$) are based on the log-likelihood ratio between both hypotheses:

$$\mathcal{S}(\mathrm{r}(k)) = \ln \frac{p_\ell(\mathrm{r}(k))}{p_0(\mathrm{r}(k))}, \tag{17}$$

where $p_\ell(\mathrm{r}(k))$ is the probability density of $\mathrm{r}(k)$ under the hypothesis $\mathcal{H}_\ell$, namely

$$p_\ell(\mathrm{r}(k)) = \frac{1}{\sqrt{(2\pi)^q \det \Sigma}} \mathrm{e}^{-\frac{1}{2}(\mathrm{r}(k)-\nu_\ell)^T \Sigma^{-1} (\mathrm{r}(k)-\nu_\ell)} \tag{18}$$

with $\nu_\ell = \nu_0$ when $\ell = 0$.

The optimal CUSUM decision function for this problem is given by (Blanke et al. 2003):

$$g(k) = \max_{1 \le j \le k} \sum_{i=j}^{k} \mathcal{S}(\mathrm{r}(i)). \tag{19}$$

The log-likelihood ratio is scalar, so the recursive computation of $g(k)$ can be performed as

$$g(k) = \max(0, g(k-1) + \mathcal{S}(\mathrm{r}(k))). \tag{20}$$

The CUSUM test is achieved by choosing an adequate detection threshold h to which the decision function $g(k)$ is compared. The choice of the threshold h results from a compromise between the mean delay for detection and the mean time between false alarms. Both quantities can be determined from the so-called average run length (ARL) function which represents the expected value of the alarm time instant for the case of detection of a change in a mean of a Gaussian sequence. Exact and approximate expressions and bounds are available and the reader should refer to Basseville and Nikiforov (1993) for more details on how to set the detection threshold h with respect to the desired mean detection delay or mean time between false alarms.

6. Implementation and diagnosis results

The results presented below correspond to the real-time implementation of the designed fuzzy FDD scheme. Five single faults (e.g. leak, sensor and actuator faults) with different magnitudes were introduced at different time instants to validate the fuzzy FDD scheme. For each fault type ℓ, $\ell = 1, \ldots, 5$, and each fault magnitude, several experiments have been conducted on the real plant in order to obtain adequate estimates of the change in the mean of the residual vector, the mean detection delay and then the detection threshold h.

First, the fault-free and the faulty data samples generated through different experiments on the real pilot plant were analysed. The residual vector used is $\mathrm{r} = [r_1\ r_2\ r_3\ r_4\ r_5\ r_6]^T$ with r_j, $j = 1, \ldots, 6$, as defined in Section 4. The estimates of the mean value $\hat{\nu}_0$ and the covariance matrix $\hat{\Sigma}$ are determined from the collected 2000 samples of this residual vector, corresponding to a healthy working mode. To simulate leaks in the water circulation pipe of the heat exchanger, a single-leak fault with magnitude 25%, 30% or 40% is introduced at time instant t using a bypass valve. On the other hand, single water and air temperature sensor faults with magnitude 1°C, 2°C or 4°C are considered by adding offsets to the measured values of T_{34} and T_{16}. To simulate actuator faults, two test cases were considered: the blockage of the air recycling valve V_r by keeping it fully closed from a given time instant and a fault on the heating power actuator by adding offsets of 1, 2 or 5 kW to P from different time instants. Some of the corresponding residual patterns are shown in Tables 4 and 5, as mentioned in Section 4.

Analysing the noisy data collected for each fault mode, we concluded that the minimum positive change in the mean value of the residual vector $\mathrm{r}(k)$ caused by a given leak flow is about 4°C. The minimum change in the mean of r(k) due to a temperature sensor fault is chosen to be $\pm 1°$C and ± 1 V (normalised value) for all actuator faults. From a practical viewpoint, these values seem to be too small, but we choose to set them in this manner, in our experimental study, in order to enlarge the sensitivity of the designed fuzzy FDD algorithm. The determined values are then used to set the constant vectors ν_ℓ, $\ell = 1, \ldots, 5$, in the CUSUM algorithm. Then, in order to determine the test threshold h, fault-free data samples of the residual vector r(k) are used. As mentioned in Section 5, the choice of the test threshold h results from a compromise between the mean delay for detection and the mean time between false alarms. In this work, h is determined using the Siegmund's approximation of the ARL function described in Basseville and Nikiforov (1993) which provides, in our case, an expectation of the alarm time instant k_a. The detection and diagnosis results for the determined values of the threshold h are presented below.

Table 6 shows the leak diagnosis results obtained for $h = 35$ and $h = 50$. Based on the ARL function, it was found that the detection threshold $h = 35$ gives an estimated mean time between false alarms larger than 10^{16} while assuring an estimated mean detection delay lower than 10 samples. One can notice that when a 25% leak fault is introduced at time instant $t = 1900$ s, a warning is provided after 40 s. This is a relatively small leak size, which means that the obtained result is very acceptable. The same situation holds when 30% and 40% leak faults are separately introduced at $t = 1280$ s and $t = 580$ s. Here, it is important to underline the good performance of the fuzzy FDD scheme which appears to be reasonable. The 30% leak fault is detected after 12 s. However, we must notice that a false alarm is generated in the last experiment at $t = 526$ s. This situation can be avoided by increasing the test threshold h. Indeed, for $h = 50$, the 40% leak is detected after 44 s with no false alarms. But in turn, this has increased slightly the detection delay which becomes 48 s for 25% leak case and 14 s for 30% leak size.

For sensor and actuator faults, the performance of the FDD algorithm is found to be very interesting when the detection threshold is chosen in the range 30–45. However, this would induce false alarms under the 40% leak fault situation, as indicated previously. For this reason, it is convenient to keep the test threshold at $h = 50$ for all fault types. The diagnosis results for different magnitudes of sensor and actuator faults are indicated in Table 7. It appears that the water temperature sensor fault is detected much more quickly than the air temperature sensor fault, due to the slow evolution of the water temperature. Overall, the obtained detection delays are all in a reasonable time range and no false alarms are recorded. This result can be interpreted as a measure for the validity and reliability of the diagnosis results.

Table 6. CUSUM-based leak diagnosis results for $h = 35$ and $h = 50$.

Leak size (%)	Occurrence time instant (s)	Alarm instant (s) $h = 35$	Alarm instant (s) $h = 50$	Detection delay (s) $h = 35$	Detection delay (s) $h = 50$	False alarms $h = 35$	False alarms $h = 50$
25	1900	1940	1948	40	48	0	0
30	1280	1292	1294	12	14	0	0
40	580	526	624	–	44	1	0

7. Conclusion

In this article, a model-based approach for FDD in a pilot co-current heat exchanger is proposed using fuzzy implications and reasoning. The fuzzy FDD scheme involves a set of TS-type fuzzy models, identified from healthy input-output observations using the well-established GK fuzzy

Table 7. CUSUM-based diagnosis results for sensor and actuator faults with $h = 50$.

Fault type	Fault magnitude	Occurrence time instant (k_0)	Alarm instant	Estimate of the occurrence instant	Detection delay (s)	False alarms
$f_{T_{34}}$	1°C	1500	1504	1486	8	0
	2°C	1500	1503	1489	6	0
	4°C	1500	1502	1489	4	0
$f_{T_{16}}$	1°C	1500	1529	1520	58	0
	2°C	1000	1012	1000	24	0
	4°C	1000	1007	1000	14	0
f_P	1 kW	650	667	652	34	0
	2 kW	500	507	502	14	0
	5 kW	500	505	503	10	0
f_V	Closed	500	510	507	20	0

clustering algorithm. The models are run in parallel to the real process for symptom generation. Leak, sensor and actuator faults with different magnitudes are considered. The detection capability of the implemented FDD algorithm is well justified through several experiments. The main advantage of the method is the use of dynamic fuzzy predictors that can be trained from measurement data instead of applying complicated first principle laws. The implementation of the proposed fuzzy FDD algorithm results in correct and early detection of different types of faults which can be interpreted as a measure for validity and reliability of the diagnosis system. Overall, it can be stated that this fuzzy reasoning based approach can be scaled up to a larger industrial heat exchangers with moderate effort and would have interesting impacts on safety and maintenance issues.

Notes on contributors

Hacene Habbi was born in Hadjout, Algeria, in 1974. He graduated in 1997 from Institut National des Hydrocarbures (INH), Algeria, in control engineering. He received his Magister and Doctorate degrees in Control Engineering, all from the University of Boumerdès, Algeria, in 2001 and 2007, respectively. He is currently an associate professor in control engineering at the Faculty of Oil and Chemistry (F.H.C.) of the University of Boumerdès, Algeria. His research interests are in the areas of intelligent systems, fuzzy modelling and control, and fault detection and diagnosis with applications to industrial processes.

Madjid Kidouche was born in Bordj-Menaiel, Algeria. Since 1992, he has been with the Department of Control Engineering, University of Boumerdès, Algeria, where his present position is associate professor of engineering. His current research interests include nonlinear control theory, fuzzy logic and large scale dynamical systems with emphasis on decomposition and aggregation, Lyapunov stability, and decentralised control.

Michel Kinnaert graduated in 1983 from Université Libre de Bruxelles (ULB), Belgium, in Mechanical and Electrical Engineering. He received his MS degree in electrical engineering from Stanford University in 1984, and his PhD degree from ULB in 1987. After being employed for 6 years by the Belgian National Fund for Scientific Research, he was appointed by ULB, where he is now professor in the Department of Control Engineering and System Analysis. He has been the chairman of the IFAC Technical Committee SAFEPROCESS from 2002 to 2008 and he has been an associate editor of the *IFAC Journal Control Engineering Practice* since 2005. His research interests include fault detection and isolation and fault tolerant control, with applications in the process industry, power systems and mechatronics.

Mimoun Zelmat was born in Algeria, in 1946. He received his PhD and Doctorate degrees in control engineering, all from Gubkine Institute of Oil and Gas of Moscow, Russia, in 1981 and 1992, respectively. He is currently the director of the Applied Automation Laboratory at the Faculty of Oil and Chemistry, University of Boumerdès. His research interests include adaptive control, intelligent modelling and control of dynamical systems and automation.

References

Astorga-Zaragoza, C.-M., Alvarado-Martinez, V.-M., Zavala-Rio, A., Mendez-Ocana, R.-M., and Guerrero-Ramrez, G.-V. (2008), 'Observer-based Monitoring of Heat Exchangers', *ISA Transactions*, 47, 15–24.

Babuška, R., Roubos, J.A., and Verbruggen, H.B. (1998), 'Identification of MIMO Systems by Input–output TS Fuzzy Models', *Proceedings of the IEEE International Conference on Fuzzy Systems*, 1, 657–662.

Babuška, R., and Verbruggen, H.B. (1996), 'An Overview of Fuzzy Modeling for Control', *Control Engineering Practice*, 4, 1593–1606.

Ballé, P. (1999), 'Fuzzy-model-based Parity Equations for Fault Isolation', *Control Engineering Practice*, 7, 261–270.

Ballé, P., and Fuessel, D. (2000), 'Closed-loop Fault Diagnosis Based on a Nonlinear Process Model and Automatic Fuzzy Rule Generation', *Engineering Applications of Artificial Intelligence*, 13, 695–704.

Ballé, P., Juricic, D., Rakar, A., and Ernst, S. (1997), 'Identification of Nonlinear Processes and Model Based Fault Isolation Using Local Linear Models', in *Proceedings of the ACC*, New Mexico, pp. 47–51.

Basseville, M., and Nikiforov, I.V. (1993), *Detection of Abrupt Changes – Theory and Applications,* Information and System Science Series. Englewood Cliffs, NJ: Prentice Hall.

Blanke, M., Kinnaert, M., Lunze, J., and Staroswiecki, M. (2003), *Diagnosis and Fault Tolerant Control*, Springer Edition, Berlin: Springer.

Cao, S., Rees, N.W., and Feng, G. (1997), 'Analysis and Design for a Class of Complex Control Systems – Part I: Fuzzy Modelling and Identification', *Automatica*, 33, 1017–1028.

Driankov, D., Hellendoorn, H., and Reinfrank, M. (1993), *An Introduction to Fuzzy Control*, Berlin: Springer.

Fink, A., Fischer, M., Nelles, O., and Isermann, R. (2000), 'Supervision of Nonlinear Adaptive Controllers Based on

Fuzzy Models', *Control Engineering Practice*, 8, 1093–1105.

Gertler, J.J. (1988), 'Survey of Model-based Failure Detection and Isolation in Complex Plants', *IEEE Control System Magazine*, 8, 3–11.

Gustafson, D.E., and Kessel, W.C. (1978), 'Fuzzy Clustering with a Fuzzy Covariance Matrix', in *Proceedings IEEE CDC*. San Diego, CA, pp. 761–766.

Habbi, H., Zelmat, M., and Ould Bouamama, B. (2003), 'A Dynamic Fuzzy Model for a Drum–Boiler–Turbine System', *Automatica*, 39, 1213–1219.

Isermann, R. (1984), 'Process Fault Detection Based on Modeling and Estimation Methods – A Survey', *Automatica*, 20, 387–404.

Isermann, R. (2005), 'Model-based Fault-detection and Diagnosis – Status and Applications', *Annual Reviews in Control*, 29, 71–85.

Johansen, A., Shorten, R., and Smith, R.M. (2000), 'On the Interpretation and Identification of Dynamic Takagi–Sugeno Fuzzy Models', *IEEE Transactions on Fuzzy Systems*, 8, 297–313.

Kinnaert, M., Vrancic, D., Denolin, E., Juricic, D., and Petrovcic, J. (2000), 'Model-based Fault Detection and Isolation for a Gas–Liquid Separation Unit', *Control Engineering Practice*, 8, 1273–1283.

Persin, S., and Tovornik, B. (2005), 'Real-time Implementation of Fault Diagnosis to a Heat Exchanger', *Control Engineering Practice*, 13, 1061–1069.

Setnes, M. (2000), 'Supervised Fuzzy Clustering for Rule Extraction', *IEEE Transactions on Fuzzy Systems*, 8, 416–424.

Simani, S., Fantuzzi, C., and Patton, R.J. (2002), *Model-based Fault Diagnosis in Dynamic Systems Using Identification Techniques*, Berlin: Springer.

Skrjanc, I., and Matko, D. (2000), 'Predictive Functional Control Based on Fuzzy Model for Heat-exchanger Pilot Plant', *IEEE Transactions on Fuzzy Systems*, 8, 705–712.

Sugeno, M., and Yasukawa, T. (1993), 'A Fuzzy-logic-based Approach to Qualitative Modeling', *IEEE Transactions on Fuzzy Systems*, 1, 7–31.

Sun, X., Chen, T., and Marquez, H. (2002), 'Efficient Model-based Leak Detection in Boiler Steam-water Systems', *Computers and Chemical Engineering*, 26, 1643–1647.

Weyer, E., Szederkenyi, G., and Hangos, K. (2000), 'Grey Box Fault Detection of Heat Exchangers', *Control Engineering Practice*, 8, 121–131.

Zhao, J., Wertz, V., and Gorez, R. (1994), 'A Fuzzy Clustering Method for the Identification of Fuzzy Models for Dynamic Systems', *International Symposium on Intelligent Control*, Ohio, USA, pp. 172–177.